The conformational behaviour and P-selectin inhibition of fluorine-containing sialyl LeX glycomimetics†

Javier Pérez-Castells,[a,c] José Juan Hernández-Gay,[a] Richard W. Denton,[b] Kurissery A. Tony,[b] David R. Mootoo*[b] and Jesús Jiménez-Barbero*[a]

Received 30th October 2006, Accepted 9th February 2007
First published as an Advance Article on the web 1st March 2007
DOI: 10.1039/b615752a

A combination of experimental *J*/NOE NMR data with molecular mechanics and dynamics calculations has been used to examine the conformational behaviour and assign the configuration of synthetically prepared epimeric 3-carboxymethyl-*O*-Gal-(1→1)-α-Man-fluoro-*C*-glycosides. It is shown that the population distributions around the glycosidic linkages strongly depend on the configuration at the fluorinated carbon of the pseudoacetal residue. It is also shown that these compounds resemble the inhibition ability of sialyl LeX towards P-selectin.

Introduction

Carbohydrate–protein interactions are involved in a wide variety of biological cell–cell recognition events such as embryogenesis, fertilization, hormonal activities and in cell proliferation and organization into specific tissues. These interactions are also involved in the invasion and attachment of pathogens, inflammation, metastasis, blood group recognition and immunology.[1] Sugar mimics that are able to bind viral and microbial surface lectins, thereby providing potential protection against infection, have recently received great synthetic and structural attention.[2] *C*-Glycosides, where the *exo* glycosidic oxygen in the natural *O*-glycosides is replaced with a methylene group, are attractive due to their chemical and enzymatic stability.[3] It is important that these compounds exhibit similar three-dimensional structures as their parent *O*-glycosides, so that the recognition process is not compromised.[4] However, the substitution of the acetal oxygen atoms by methylene groups results in changes in the flexibility and population distributions around the inter-residue linkages. In particular we have shown that *C*-analogues are rather more flexible than the natural compounds, possibly because of the absence of the *exo*-anomeric effect,[5] and may access a larger variety of conformations. Nevertheless, this greater flexibility may lead to an increase in affinity if there is an enthalpic gain that exceeds the entropic penalty. However, in cases where the bound conformation resembles the ground state of the *O*-glycoside, *C*-glycosides with close conformational behaviour to *O*-glycosides would be desirable, and, in principle, we guessed that this could be achieved by introducing substituents in the methylene link.[6] Sialyl Lewis X (sLe^x) is a terminal tetrasaccharide expressed on the surface of tumor cells and neutrophils and its interaction with the selectins has been associated with cancer metastasis and inflammation disorders. Among the drawbacks with advancement of sLe^x as a drug are its relatively weak selectin binding, the high cost of synthesis and its poor bioavailability.[7] Accordingly, relatively simple mimics like the α-*O*-Gal-(1,1)-β-Man **1**, which we recently found to be similar in activity to sLe^x in a P-selectin binding assay, have attracted attention.[8] The disaccharide of residue **1** presumably acts as a replacement for the Gal-GlcNAc-Fuc trisaccharide of sLe^x, and the carboxymethyl group incorporated into the 3-OH group of the galactose segment plays the role of the sialic acid. The *C*-glycosyl analogue **2** is of interest as a potential therapeutic agent because of its hydrolytic stability, and its conformational properties may be of relevance to structure–activity studies. We have previously shown that **2** is more flexible than **1** with respect to the intersaccharide torsions.[5] Herein, using a protocol based on a combination of NMR spectroscopy and molecular mechanics and dynamics calculations, we have investigated the conformational behaviour of epimers **3** and **4**[9]—analogues of **2** with a fluorine substituent in the pseudoglycoside position (Fig. 1)—and applied this information to unambiguously

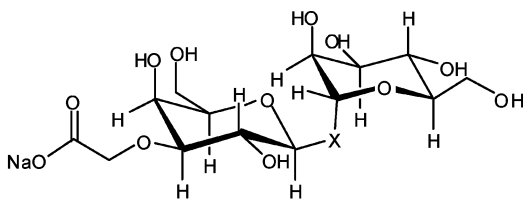

1, X = O. **2**, X = CH_2

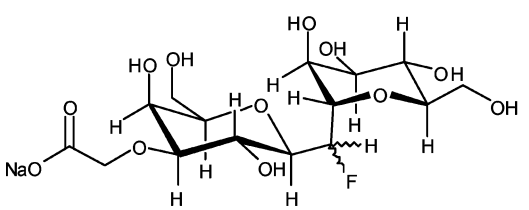

3, 4

Fig. 1 Structures of **1–4**.

[a]*Centro de Investigaciones Biológicas, CSIC, Ramiro de Maeztu 9, 28040 Madrid, Spain. E-mail: jjbarbero@cib.csic.es; Fax: +34 915531706; Tel: +34 918373112 ext. 4370*
[b]*Department of Chemistry, Hunter College, CUNY, 695 Park Avenue, New York, NY 10021, USA, dmootoo@hunter.cuny.edu; Tel: +1 212-772-4356*
[c]*Department of Chemistry, Facultad de Farmacia; Universidad San Pablo CEU, Urb Montepríncipe, 28668 Boadilla del Monte, Spain. E-mail: jpercas@ceu.es*

† Electronic supplementary information (ESI) available: P-Selectin inhibition assay data. See DOI: 10.1039/b615752a

assign their configuration. It is shown that the conformational distribution around the glycosidic linkages of **3** and **4** is very different. In addition, evaluation of these compounds in a P-selectin binding assay indicated that the analogue with a major population of the *exo*-anomeric conformation with respect to the galactose residue was approximately two-fold more active than that showing an almost negligible presentation of this geometry.

Results and discussion

Molecular modeling studies

At the onset, the configuration at the fluorinated carbon in **3** and **4** was not known. The potential energy surfaces for both epimers were calculated using the MM3*[10] force field, as previously described (Fig. 2).[11–13] These maps are useful to delimit the low-energy regions that are accessible to rotation around the glycosidic torsion angles Φ_{Gal} ($H1_{Gal}$–$C1_{Gal}$–X–$C1_{Man}$) and Φ_{Man} ($H1_{Man}$–$C1_{Man}$–X–$C1_{Gal}$). Five principal low-energy conformer types were obtained for both the *R* and *S* epimers, but with very different populations: (**A**) *exo*-Φ_{Gal}/non-*exo*-Φ_{Man}, (**B**) *exo*-Φ_{Gal}/*exo*-Φ_{Man}, (**C**) non-*exo*-Φ_{Gal}/*exo*-Φ_{Man}, (**D**) *anti*-Φ_{Gal}/non-*exo*-Φ_{Man}, (**E**) *anti*-Φ_{Gal}/*exo*-Φ_{Man}. These conformations are shown in Fig. 3, and their geometries and relative energies summarized in Table 1. The different conformers have been dubbed, *exo*, non-*exo* and *anti* with respect to glyconic torsions Φ_{Gal} and Φ_{Man}, by analogy with the *exo*-anomeric notation for *O*-glycosides. Thus *exo*-Φ_{Gal} and *exo*-Φ_{Man} correspond to values of *ca.* +60° and −60° respectively, non-*exo*-Φ_{Gal} and non-*exo*-Φ_{Man} to −60° and +60° respectively, and *anti*-Φ_{Gal} and *anti*-Φ_{Man} to 180°. For the *S* epimer, the "natural" conformer **B**, with the double *exo*-anomeric orientation, is the major one (*ca.* 40%) followed by non-*exo*-Φ_{Gal}/non-*exo*-Φ_{Man} (28%), *anti*-Φ_{Gal}/*exo*-Φ_{Man} (15%) and *anti*-Φ_{Gal}/non-*exo*-Φ_{Man} (12%). For the *R* epimer, according to

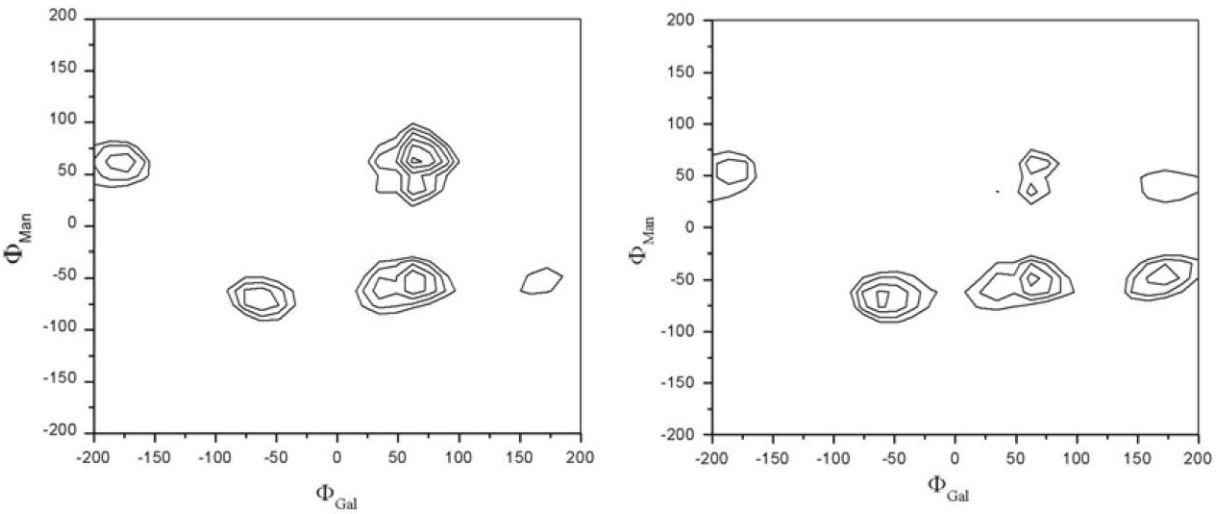

Fig. 2 Steric energy maps (Φ_{Man}, Φ_{Gal}) calculated by MM3* with $\varepsilon = 80$. Left, *R*; right, *S*. Contours are given every 2.5 kJ mol^{-1}.

Table 1 Comparison between the inter-residue proton–proton distances calculated by MM3* for the conformers **A–E** of the *R* and *S* epimers (approximate Φ_{Gal} and Φ_{Man} angles in parentheses), and the observed NOEs in the NOESY spectrum at 600 ms mixing time (S, strong; M, medium; W, weak; VW, very weak) for **3** and **4**. In all cases, NOEs or ROEs were positive, *i.e.* the cross peaks showed different sign to the diagonal peaks, as expected for small molecules. Relative steric energies for *R* and *S* epimers (ΔE, kJ mol^{-1}) are also given. Interproton distances corresponding to exclusive NOEs[12] of the *R* or *S* epimers are shown in bold. Nevertheless, for two interproton distances, *i.e.*, CHF–3M and CHF–5M, two different conformers, **A** and **D**, show short interproton distances and may explain the observed NOEs

Conformer (Φ_{Gal}/Φ_{Man})			**A**(60/60) *exo*/non-*exo*	**B**(50/−50) *exo*/*exo*	**C**(−70/70) non-*exo*/non-*exo*	**D**(−170/60) *anti*/non-*exo*	**E**(180/−70) *anti*/*exo*
ΔE (*R* isomer)	—	—	0.0	0.97	4.17	5.74	10.54
ΔE (*S* isomer)	—	—	3.57	0.0	0.54	5.14	2.72
	(**3**) NOE exp. (%)/distance	(**4**) NOE exp. (%)/distance	calc. distance *R*/*S*	calc. distance *R*/*S*	calc. distance *R*/*S*	calc. distance *R*/*S*	calc. distance *R*/*S*
1G–1M	—	—	3.15	**2.47**	3.39	3.85	3.83
1G–2M	S (13)/2.30	—	**2.28**	4.35	4.78	3.96	4.77
1G–3M	Overlap	Overlap	3.45	5.16	4.40	4.28	4.89
1G–5M	Overlap	Overlap	4.54	4.28	**2.49**	4.59	4.13
CHF–2G	M (3)/3.16	M (3)/3.07	3.14/3.24	3.18/**2.57**	**2.53**/4.06	3.81/3.24	3.85/3.18
CHF–2M	M (2)/3.19	M (3)/3.07	3.17/3.13	2.49/3.27	2.69/3.02	3.37/3.90	2.45/2.90
CHF–3M	S (13)/2.32	MS (7)/2.66	**2.44**/2.36	3.36/2.49	3.73/2.42	**2.51**/4.05	3.43/2.39
CHF–5M	Overlap	S (11)/2.47	**2.34**/2.20	4.02/2.32	4.06/2.39	**2.11**/2.94	3.86/2.51
1M–2G	VW (0.5)/4.00	M (4)/3.03	4.35	4.71	3.00	**2.52**	3.28
1M–3G	—	—	5.42	5.13	4.95	5.10	5.53
1M–5G	—	—	3.98	4.14	5.48	5.44	4.75
2M–G2	—	—	5.02	5.34	4.82	**2.73**	5.11

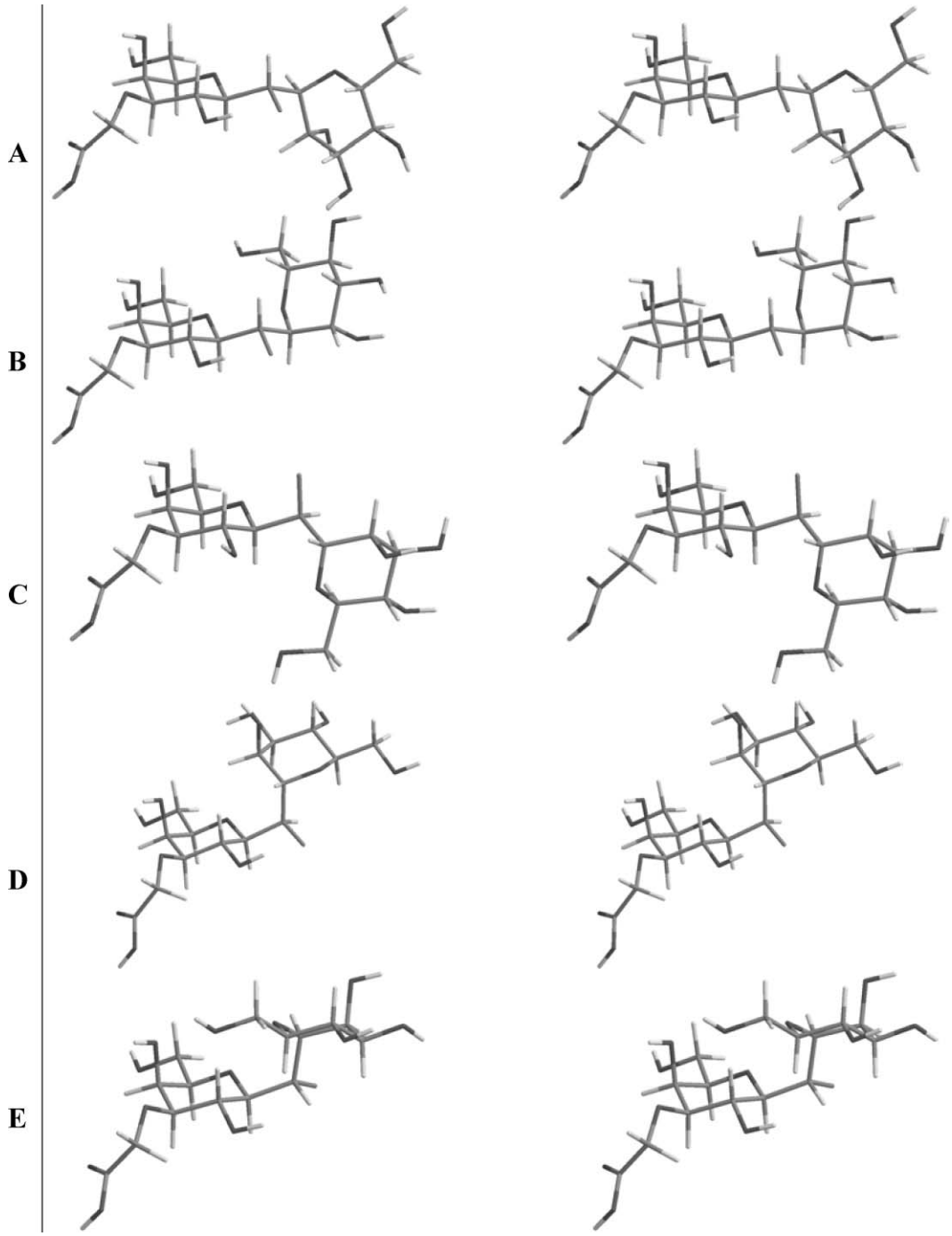

Fig. 3 Stereoviews of the global and local minima of *R* and *S* epimers according to MM3* calculations. (A) Conformer **A**; (B) conformer **B**; (C) conformer **C**; (D) conformer **D**; (E) conformer **E**. See Table 1 for the Φ_{Gal} and Φ_{Man} torsions of the different conformers.

MM3*, the major conformer is not the natural one, but the *exo*-Φ_{Gal}/non-*exo*-Φ_{Man} (65%) followed by the double *exo* conformer (26%), and very minor contributions of **C**, **D** and **E**. In addition, the conformational stability of the different conformers of both epimers was checked by using MD simulations,[14] also with the MM3* force field. Some of the computed Φ_{Man}/Φ_{Gal} distributions are displayed in Fig. 4.

Examination of proton–proton distances for the *R*/*S* epimers of the five different conformational families reveals several values of close to 2.5 Å that are exclusive to one (or a maximum of two) conformations of the *R* or *S* epimers. Observation of a NOE[15] corresponding to any of these distances could indicate the presence of the associated geometries and may be also helpful in the assignment of the yet unknown *R*/*S* configuration. These exclusive NOEs are shown in bold in Table 1.

Experimental confirmation of modeling data by NMR

The predictions from the force field calculations were compared with the experimental data as determined from NMR to deduce

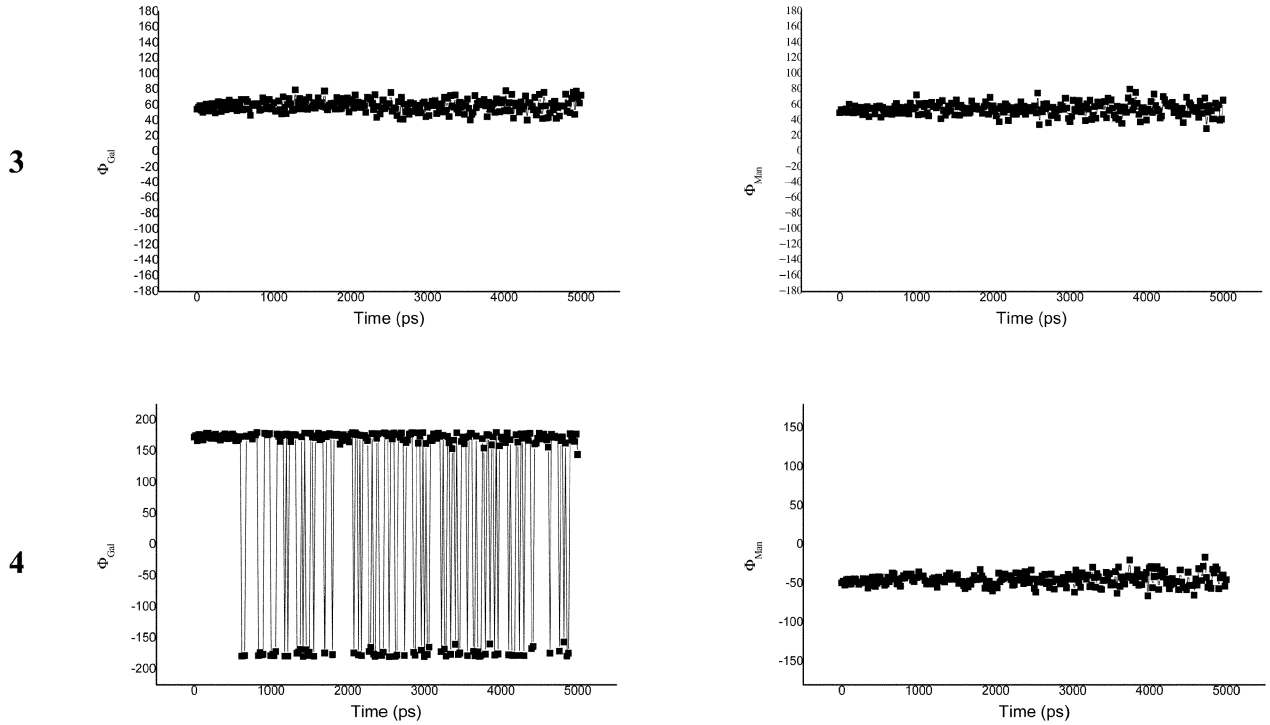

Fig. 4 Frequency of sampling of Φ_{Gal}/Φ_{Man} torsion angles from the MD simulations (MM3*) for *R* (top) and *S* (bottom) epimers.

the stereochemical assignment and final conformational distribution for **3** and **4**. The chemical shifts in D_2O are listed in Table 2. The assignment of the resonances was made through a combination of COSY, TOCSY, 1D and 2D-NOESY/ROESY, and HSQC experiments.

The *J* values for the ring protons indicate that all the pyranose chairs adopt the usual $^4C_1$ chair, independent of the size of the molecule and of the nature of the *C*- or *O*-glycosidic linkage (Table 3). The intermediate observed values for the C5–C6 lateral chains are in agreement with equilibria between the tg:gt conformers for the Gal/pseudoGal rings and the gg:gt conformers for the Man moieties.[16]

Table 2 ^{1}H NMR chemical shifts (δ, ppm) and vicinal coupling constants (*J*, Hz) for compounds **3** and **4**

Comp.	**3** δ/ppm (*J*/Hz)	**4** δ/ppm (*J*/Hz)
H1M	4.32 (16.30, 8.69)	4.34 (15.43, 7.02)
H2M	3.97	4.21
H3M	3.65	3.84 (8.78)
H4M	3.62	3.63
H5M	3.66	3.58
H6aM	3.82 (−12.0)	3.80 (−12.04)
H6bM	3.72	3.64
CHF	5.13 (47.55, 8.61)	5.09 (46.51, 6.98)
H1′G	3.39 (29.75, 10.3)	3.68
H2′G	3.93 (10.3)	3.89
H3′G	3.45 (9.56)	3.42 (8.88)
H4′G	4.07	4.06
H5′G	3.61	3.61
H6′aG	3.72	3.71 (−12.04)
H6′bG	3.66	3.69

Table 3 Expected *J* values (Hz) for the basic conformations around Φ_{Gal} and Φ_{Man} angles for *R* and *S* analogues, deduced by applying the generalized Karplus[17a] equation proposed by Altona[17b] to the geometries provided by MM3* molecular mechanics calculations, and by applying the Karplus-type equation for the $J_{H,F}$ constants[18]

	Expected for conformer (*J*/Hz)					Exp. (*J*/Hz)	
Atom pair	**A**	**B**	**C**	**D**	**E**	**3**	**4**
R epimer							
G-1′H/C*H*F	0.4	−0.3	7.9	4.7	4.2	<1	<1
G-1′H/F	34.2	36.2	15.1	12.2	16.2	29.6	overlap
M-1H/C*H*F	9.7	−0.4	0.8	8.0	0.4	8.6	7.1
M-1H/F	11.0	35.9	30.1	14.5	36.1	16.3	15.4
S epimer							
G-1′H/C*H*F	9.5	9.5	0.8	2.9	3.3	<1	<1
G-1′H/F	8.3	11.0	33.5	14.5	14.5	29.6	overlap
M-1H/C*H*F	0.8	9.5	8.7	0.8	9.5	8.6	7.0
M-1H/F	32.1	11.0	14.5	33.5	15.0	16.3	15.4

In a second step, NOESY and ROESY experiments were carried out to determine the intensities of the observed NOEs. Experimental proton–proton distances were obtained as described in the experimental section and compared to those estimated by the MM3* molecular mechanics and dynamics calculations (Table 1). Experimental and calculated interglycosidic *J* values between the proton or the fluorine attached to the intersaccharide bridge and H-1Gal and H-1Man at the pseudoanomeric carbons were also obtained (Table 3). The Karplus-type equation developed by Chattopadhyaya was used for the theoretical values of the $J_{H,F}$ constants.[18]

Comparison of the calculated H,H[17a] and H,F coupling constants for compound **3** with the corresponding *J* values for the geometries obtained from molecular mechanics, suggests that the

possibilities for the major conformer population of **3** are the *exo*-Gal/non-*exo*-Man conformer (*i.e.* **A**) of epimer *R*, or the non-*exo*-Φ_{Gal}/*exo*-Φ_{Man} (*i.e.* **C**) of epimer *S*. However, the observation of a strong 1G–2M NOE, which is exclusive for conformer **A**, and is not predicted for **C**, points to the *R*-epimer/conformer **A** over the *S*-epimer/conformer **C**. This assignment is supported by the observation of a NOE between CHF and 3M which is also expected for the *R*-epimer/conformer **A**. A CHF–3M NOE is also predicted for conformer **D** but a major contribution from this conformer is unlikely, considering the weakness of the 1M–2G NOE and the absence of 2M–2G, both of which are exclusive NOEs for **D**. Therefore, compound **3** is the *R* epimer and on the basis of *J* value analysis exists predominantly as a *non-natural* conformer[19] with a major non-*exo*-anomeric conformation around the Φ_{Man} glycosidic linkage, *i.e.*, the *exo*-Gal/non-*exo*-Man conformer (90%), with a minor contribution from the *natural exo*-Gal/*exo*-Man conformer (<10%). Thus, the *exo*-Gal/*exo*-Man conformer for epimer *R* seems to be largely overestimated by the MM3* simulations within MACROMODEL[20] (from 24% to less than 10%). The absence of the 1G–1M NOE, which is predicted to be strong for conformer **B** is consistent with this conclusion.

Due to signal overlapping, only three of the four vicinal *J* values were discernible for compound **4**. Since these are very similar to the corresponding values for **3**, the same two possibilities, *i.e. R*-epimer/conformer **A** and *S*-epimer/conformer **C** may be considered. However, the lack of information for $J_{G1H/CHF}$ requires that a third scenario, *S*-epimer/conformer **E** (*anti*-Φ_{Gal}/*exo*-Φ_{Man}) be entertained. The absence of an exclusive NOE for **B** (and **A**) weighs against the possibility of **4** being the *R*-epimer/conformer **A**. While the absence of a NOE does not generally exclude the possibility of the associated conformation, the fact that the 1G–2M NOE is not observed at all for **4** (whereas it is for **3**), is more in line with *S*-epimer/conformer **C** and/or *S*-epimer/conformer **E** than *R*-epimer/conformer **A**. Strong CHF–3M and CHF–5M NOEs support the presence of both conformers **C** and **E** but an estimate of the conformer ratio is not possible because the experimentally available *J* values for **4** are very similar to predicted data for **C** and **E**. The observed *J* values do, however, rule out the presence of **A**, **B**, and **D**. In any event, as is the case for the *R*-epimer, the stability of the *exo*-Gal/*exo*-Man conformer for epimer *S* is also overestimated by the MM3* simulations. Therefore, the conformational behaviour of **3** (*R*-epimer) and **4** (*S*-epimer) is very different from each other, and from that of the parent *O*-glycoside. The basis for these differences is presumably rooted in steric and polar effects and remains to be investigated.

The interaction with P-selectin

The interaction of **3** and **4** with P-selectin was evaluated using a soluble truncated form of human P-selectin in a Biacore assay with an immobilized monomeric truncated form of human PSGL-1 as the reference ligand.[21] At 6 and 12 mM, **3** showed 19 and 39% inhibition respectively, and **4** showed 13 and 26% inhibition respectively. *O*-Glycoside **1** exhibits 33 and 48% inhibition at these concentrations, which is similar to the activity that was previously noted for sLe^x in the Biacore assay.[8,21] Unfortunately, the similar activity of **1**, **3** and **4** does not allow for any clear structure–activity conclusions. Nevertheless, it is noteworthy that **1** and **3**, which both exist mainly (>90%) as *exo*-Gal rotamers, are clearly more active than **4**, which does not appear to have an appreciable population of this "natural" orientation.

Conclusions

As described in earlier studies,[5] the conformational distributions around the glycosidic linkages of the parent *O*-glycoside **1** and its *C*-glycoside analogue **2** are rather different. **1** populates almost entirely (>93%) the natural *exo*-Gal/*exo*-Man (**B**) conformation, whereas **2** is very flexible and exists in this conformation in only 30% population, with four other conformational families, **A** (42%), **C** (6%), **D** (10%) and **E** (12%), present in solution.[5] The present investigation indicates that their fluorinated analogues also show rather distinct conformational features. The *R*-fluoro-*C*-glycoside **3** exists predominantly as *exo*-Gal/non*exo*-Man conformer **A** (*ca.* 90%) with a minor population of **B**. The result for the *S*-fluoro-*C*-glycoside **4** is not as conclusive, but it appears that this analogue populates mainly non-natural conformers **C** and/or **E**. With respect to their interaction with P-selectin both *C*-fluoro disaccharides showed similar activity as the parent *O*-disaccharide. In view of the very different conformational preferences, the similar activity of these three analogues might be an indication that they are not preorganized in an optimal conformation for binding, and all incur similar energetic penalties in so doing. It is possible that fluoro-*C*-glycoside mimics like **3** and **4** would provide more meaningful structure–activity information in cases where the glycosidic oxygen of the parent *O*-glycoside interacts directly with the receptor. This is an avenue for future investigation.

Experimental

General

The synthesis of these compounds has been described elsewhere.[9]

Molecular modeling

Potential energy surfaces and population maps were calculated using the MM3* force field,[10] as implemented in MACROMODEL 7.1.[20] The torsion angle Φ_{Man} is defined as H1Man–C1Man–*C*HF–C1Gal and Φ_{Gal} as H1Gal–C1Gal–*C*HF–C1Man. In a first step, a rigid Φ_{Gal}/Φ_{Man} map was calculated by using a grid step of 18° at each torsion coordinate.[22,23] The corresponding 400 conformers were optimized by fixing Φ_{Gal}/Φ_{Man} at each corresponding value to generate the relaxed energy map. The probability distribution was calculated from the energy values according to a Boltzmann function at 300 K. In all the molecular mechanics and dynamics calculations, the GB/SA solvation model for water was used.

The molecular dynamics simulations were also performed using the MM3* force field within MACROMODEL 7.1. For molecular dynamics simulations, several geometries, corresponding to the different low energy minima, were used as input. A temperature of simulation of 300 K was employed with a time step of 1.5 fs and an equilibration time of 100 ps. The total simulation time for each compound was 5 ns.

NMR spectroscopy

^{1}H-NMR (500 MHz) spectra were recorded at 30 °C in D_2O, on a Bruker DRX 500 spectrometer. Concentrations of *ca.* 5 mM of

3 and **4** were used. Chemical shifts are reported in ppm, using external TMS (0 ppm) as reference. The 2D-TOCSY experiment (70 ms mixing time) was performed using a data matrix of 256 × 2 K to digitize a spectral width of 3000 Hz. Four scans were used per increment with a relaxation delay of 2 s. 2D-NOESY (600, 800 and 1000 ms) and 2D-T-ROESY experiments (300, 400 and 500 ms) used the standard sequences. 1D-Selective NOE spectra were acquired using the double echo sequence proposed by Shaka and co-workers[24] at 250, 350, 450, and 550 ms of mixing time. Distances were estimated from NOESY/ROESY experimental data as follows: NOE intensities were normalized with respect to the diagonal peak at zero mixing time. Selective T_1 measurements were performed on the anomeric and several other protons to obtain the values indicated in Table 1. Experimental NOEs were fitted to a double exponential function, $f(t) = p0(e^{-p1t})(1 - e^{-p2t})$ with $p0$, $p1$ and $p2$ being adjustable parameters.[5] The initial slope was determined from the first derivative at time $t = 0$, $f'(0) = p0p2$. From the initial slopes, interproton distances were obtained by employing the isolated spin pair approximation.

All the theoretical NOE calculations were automatically performed by a home-made programme, which is available from the authors upon request.[22,23]

P-Selectin inhibition assay

P-Selectin inhibition assays for **3** and **4** were performed using a surface plasmon (Biacore) assay on a Biacore 3000 instrument, following the published protocol.[21] Biotinylated 19ek (a purified monomeric truncated form of human PSGL-1) was immobilized on SA sensor chip 11 and a soluble recombinant truncated form of human P-selectin was delivered to the coated 19ek sensor chip at 30 μL min^{-1} and 25 °C in the presence or absence of the test ligand (see supporting information†).

Acknowledgements

We thank Dirección General de Investigación of Spain (BQU2003-03550-C03-01), and the National Institutes of Health (R01-GM57865), for funding. "Research Centers in Minority Institutions" award RR-03037 from the National Center for Research Resources of the NIH, which supports the infrastructure and instrumentation of the Chemistry Department at Hunter College, and MBRS–RISE award GM60665, are also acknowledged. JPC acknowledges Fundación San Pablo CEU for sabbatical leave.

References

1 (*a*) H.-J. Gabius, H.-C. Siebert, S. André, J. Jiménez-Barbero and H. Rüdiger, *ChemBioChem*, 2004, **5**, 740–764; (*b*) T. K. Dam and C. F. Brewer, *Chem. Rev.*, 2002, **102**, 387–429; (*c*) H.-J. Gabius, S. André, H. Kaltner and H.-C. Siebert, *Biochim. Biophys. Acta*, 2002, **1572**, 165–177; (*d*) C. R. Bertozzi and L. L. Kiessling, *Science*, 2001, **291**, 2357; (*e*) *Glycosciences: Status and Perspectives*, ed. H.-J. Gabius and S. Gabius, Chapman and Hall, London, Weinheim, 1997; (*f*) H. Rüdiger, H.-C. Siebert, D. Solís, J. Jiménez-Barbero, A. Romero, C.-W. von der Lieth, T. Diaz-Mauriño and H.-J. Gabius, *Curr. Med. Chem.*, 2000, **7**, 389–416.

2 (*a*) S. J. Danishefsky and J. R. A. Allen, *Angew. Chem., Int. Ed.*, 2000, **39**, 836; (*b*) Z. J. Witczak, *Curr. Med. Chem.*, 1999, **6**, 165.

3 For instance, see: (*a*) R. V. Weatherman and L. L. Kiessling, *J. Org. Chem.*, 1996, **61**, 534; (*b*) R. V. Weatherman, K. H. Mortell, M. Chervenak, L. L. Kiessling and E. J. Toone, *Biochemistry*, 1996, **35**, 3619; (*c*) L. M. Mikkelsen, M. J. Hernáiz, M. Martín-Pastor, T. Skrydstrup and J. Jiménez-Barbero, *J. Am. Chem. Soc.*, 2002, **124**, 14940–14951.

4 (*a*) M. S. Searle and D. H. Williams, *J. Am. Chem. Soc.*, 1992, **114**, 10690–10697; (*b*) H.-J. Gabius, *Pharm. Res.*, 1998, **15**, 23–30; (*c*) T. K. Dam and C. F. Brewer, *Chem. Rev.*, 2002, **102**, 387–429.

5 (*a*) J. L. Asensio, F. J. Cañada, X. Cheng, N. Khan, D. R. Mootoo and J. Jiménez-Barbero, *Chem.–Eur. J.*, 2000, **6**, 1035–1041; (*b*) V. García-Aparicio, M. C. Fernández-Alonso, J. Angulo, J. L. Asensio, F. J. Cañada, J. Jiménez-Barbero, D. R. Mootoo and X. Cheng, *Tetrahedron: Asymmetry*, 2005, **16**, 519–527.

6 J. F. Espinosa, M. Bruix, O. Jarreton, T. Skrydstrup, J.-M. Beau and J. Jiménez-Barbero, *Chem.–Eur. J.*, 1999, **5**, 442–448.

7 (*a*) G. Bendas, *Mini-Rev. Med. Chem.*, 2005, **5**, 575–584; (*b*) N. Kaila and B. E. Thomas IV, *Med. Res. Rev.*, 2002, **22**, 566–601; (*c*) G. J. McGarvey, J. A. Jablonowski and C.-H. Wong, *Chem. Rev.*, 1998, **98**, 833–862.

8 R. W. Denton, X. Cheng, K. A. Tony, A. Dilhas, J. J. Hernández, A. Canales, J. Jiménez-Barbero and D. R. Mootoo, *Eur. J. Org. Chem.*, 2007, 645–654. Earlier measurements in a cell based assay indicated **1** to be 5 times and 40 times as active as sLe^x in binding to E- and P-selectin respectively: K. Hiruma, T. Kajimoto, G. Weitz-Schmidt, I. Ollmann and C.-H. Wong, *J. Am. Chem. Soc.*, 1996, **118**, 9265–9270; K. Shibata, K. Hiruma, O. Kanie and C.-H. Wong, *J. Org. Chem.*, 2000, **65**, 2393–2398.

9 Compounds **3** and **4** were prepared following a variation of the methodology described for **2**: N. Khan and D. R. Mootoo, *J. Org. Chem.*, 2000, **65**, 2544–2547. Their syntheses will be described elsewhere: K. A. Tony, R. W. Denton, A. Dilhas, J. Jiménez-Barbero and D. R. Mootoo, *Org. Lett.*, in press.

10 (*a*) D. A. Pearlman, D. A. Case, J. W. Caldwell, W. S. Ross, T. E. Cheatham, S. DeBolt, D. Ferguson, G. Seibel and P. Kollman, *Comput. Phys. Commun.*, 1995, **91**, 1–41; (*b*) N. L. Allinger, Y. H. Yuh and J.-H. Lii, *J. Am. Chem. Soc.*, 1989, **111**, 8551–8559.

11 (*a*) H.-J. Gabius, F. Darro, M. Remmelink, S. André, J. Kopitz, A. Danguy, S. Gabius, I. Salmon and R. Kiss, *Cancer Invest.*, 2001, **19**, 114–126; (*b*) H.-J. Gabius, *Biochimie*, 2001, **83**, 659–666.

12 See, for instance: J. L. Asensio, J. F. Espinosa, H. Dietrich, F. J. Cañada, R. R. Schmidt, M. Martín-Lomas, S. André, H.-J. Gabius and J. Jiménez-Barbero, *J. Am. Chem. Soc.*, 1999, **121**, 8995–9000.

13 For instance, see: (*a*) A. Poveda, J. L. Asensio, T. Polat, H. Bazin, R. J. Linhardt and J. Jiménez-Barbero, *Eur. J. Org. Chem.*, 2000, 1805–1813; (*b*) E. Montero, A. García-Herrero, J. L. Asensio, K. Hirai, S. Ogawa, F. Santoyo-González, F. J. Cañada and J. Jiménez-Barbero, *Eur. J. Org. Chem.*, 2000, 1945, and references cited therein.

14 For a discussion on the application of molecular mechanics force fields to sugar molecules, see: S. Pérez, A. Imberty, S. B. Engelsen, J. Gruza, K. Mazeau, J. Jiménez-Barbero, A. Poveda, J. F. Espinosa, B. P. van Eyck, G. Johnson, A. D. French, M. L. C. E. Kouwijzer, P. D. J. Grootenuis, A. Bernardi, L. Raimondi, H. Senderowitz, V. Durier, G. Vergoten and K. Rasmussen, *Carbohydr. Res.*, 1998, **314**, 141–155.

15 D. Neuhaus and M. P. Williamson, *The Nuclear Overhauser Effect in Structural and Conformational Analysis*, VCH, New York, 1989.

16 K. Bock and J. O. Duus, *J. Carbohydr. Chem.*, 1994, **13**, 513–543.

17 (*a*) M. Karplus, *J. Chem. Phys.*, 1959, **30**, 11; (*b*) C. A. G. Hasnoot, F. A. A. M. de Leeuw and C. Altona, *Tetrahedron*, 1980, **36**, 2783–2792.

18 C. Thibaudeau, J. Plavec and J. Chattopadhyaya, *J. Org. Chem.*, 1998, **67**, 4967–4984.

19 J. F. Espinosa, F. J. Cañada, J. L. Asensio, M. Martín-Pastor, H. Dietrich, M. Martín-Lomas, R. R. Schmidt and J. Jiménez-Barbero, *J. Am. Chem. Soc.*, 1996, **118**, 10862–10871.

20 F. Mohamadi, N. G. J. Richards, W. C. Guida, R. Liskamp, C. Caufield, G. Chang, T. Hendrickson and W. C. Still, *J. Comput. Chem.*, 1990, **11**, 440–467.

21 N. Kaila, W. S. Somers, B. E. Thomas, P. Thakker, K. Janz, S. DeBernardo, S. Tam, W. J. Moore, R. Yang, W. Wrona, P. W. Bedard, D. Crommie, J. C. Keith, Jr., D. H. H. Tsao, J. C. Alvarez, H. Ni, E. Marchese, J. T. Patton, J. L. Magnani and R. T. Camphausen, *J. Med. Chem.*, 2005, **48**, 4346–4357.

22 J. F. Espinosa, M. Martín-Pastor, J. L. Asensio, H. Dietrich, M. Martín-Lomas, R. R. Schmidt and J. Jiménez-Barbero, *Tetrahedron Lett.*, 1995, **36**, 6329–6332.

23 J. L. Asensio, M. Martín-Pastor and J. Jiménez-Barbero, *Int. J. Biol. Macromol.*, 1995, **17**, 137–148.

24 K. Stott, J. Stonehouse, J. Keeler, T. L. Hwang and A. J. Shaka, *J. Am. Chem. Soc.*, 1995, **117**, 4199–4200.

